AIMS Geosciences

AIMS Geosciences, 9(1): 1–15.
DOI: 10.3934/geosci.2023001
Received: 11 August 2022
Revised: 01 October 2022
Accepted: 20 October 2022
Published: 03 November 2022

http://www.aimspress.com/journal/geosciences

Research article

Relationship between synoptic circulations and the spatial distributions of rainfall in Zimbabwe

Chibuike Chiedozie Ibebuchi[1, 2, *] and Itohan-Osa Abu[3]

[1] Department of Geography, Kent State University, Kent, USA
[2] Julius-Maximilians-University of Würzburg, Institute of Geography and Geology, Department of Physical Geography, Am Hubland, 97074 Würzburg, Germany
[3] Julius-Maximilians-University of Würzburg, Institute for Geography and Geology, Department of Remote Sensing, 97074 Würzburg, Germany

* **Correspondence:** Email: chibuike.ibebuchi@uni-wuerzburg.de.

Abstract: This study examines how the atmospheric circulation patterns in Africa south of the equator govern the spatial distribution of precipitation in Zimbabwe. The moisture circulation patterns are designated by an ample set of eight classified circulation types (CTs). Here it is shown that all wet CTs over Zimbabwe features enhanced cyclonic/convective activity in the southwest Indian Ocean. Therefore, enhanced moisture availability in the southwest Indian Ocean is necessary for rainfall formation in parts of Zimbabwe. The wettest CT in Zimbabwe is characterized by a ridging South Atlantic Ocean high-pressure, south of South Africa, driving an abundance of southeast moisture fluxes, from the southwest Indian Ocean into Zimbabwe. Due to the proximity of Zimbabwe to the Agulhas and Mozambique warm current, the activity of the ridging South Atlantic Ocean anticyclone is a dominant synoptic feature that favors above-average rainfall in Zimbabwe. Also, coupled with a weaker state of the Mascarene high, it is shown that a ridging South Atlantic Ocean high-pressure, south of South Africa, can be favorable for the southwest movement of tropical cyclones into the eastern coastal landmasses resulting in above-average rainfall in Zimbabwe. The driest CT is characterized by the northward track of the Southern Hemisphere mid-latitude cyclones leading to enhanced westerly fluxes in the southwest Indian Ocean, limiting moist southeast winds into Zimbabwe.

Keywords: moisture circulation; mid-latitude cyclone; southwest Indian Ocean; tropical cyclone; South Atlantic Ocean anticyclone

1. Introduction

Zimbabwe is a country in southern Africa; it is bordered by Botswana to the southwest, Mozambique to the east, South Africa to the south, and Zambia to the northwest. According to Ref [1], the estimated population in Zimbabwe is 13 million people. The climate in Zimbabwe is mainly semi-arid and rainfall in the region exhibits spatial and temporal variability [2]. Ref [3] reported that extreme rainfall and drought events have increased in intensity and frequency in Zimbabwe. Up to eighty percent of Zimbabwe's water is used in the agricultural sector [4], and Ref [5] noted that the heavy dependency of Zimbabwe on rain-fed agriculture makes it vulnerable to climate change. Further, under greenhouse-gas-induced climate change, increasing temperature and rainfall variability are expected to aggravate the decline in agricultural products [6]. Moreover, Ref [7] highlighted that drought and flooding conditions have contributed to about half of Zimbabwe's population plunging into poverty. Among other factors, inadequate specialist skills in climate change and climate predictions are some issues facing Zimbabwe in tackling climate change [5,8]. Therefore, this study aims to enhance the physical predictability of rainfall in Zimbabwe by characterizing synoptic conditions and the associating moisture flux patterns that govern the spatial distribution of rainfall over Zimbabwe. Hence the findings in this study can be used as a base material for a local weather agency.

Large parts of Southern Africa receives most of its rainfall during austral summer (DJF) and the South Indian Ocean Convergence Zone (SICZ) is the major synoptic feature that modulates the regional austral summer rainfall variability [9–11]. The SICZ is a diagonally oriented convergence zone associated with a region of enhanced precipitation that extends off the southeast coast of southern Africa. Ref [9] explained that in addition to continental heating, the convergence of moist southeast winds resulting from the anticyclonic circulation at the South Indian Ocean high-pressure, and moist northwest winds resulting from the cyclonic circulation at the Angola low form the foundation zone of the SICZ. According to Ref [12], the SICZ is related to the Inter-Tropical Convergence Zone (ITCZ) through the Angola low—an enhancement of the ITCZ can lead to the sustenance of the Angola low.

The ITCZ which is the principal large-scale feature that modulates the hydroclimate of the tropics tracks southward during austral summer so that the semi-permanent subtropical high-pressure systems are located more southward. Austral summer is equally characterized by enhanced moisture uptake at the southwest Indian Ocean, which is the principal source of moisture that is advected to southern Africa [13,14]. Warmer sea surface temperature (SST) in the southwest Indian Ocean coupled with enhanced moisture transport by southeast winds co-occurs with above-average rainfall in southern Africa [15]. Other synoptic features such as cut-off lows and the Mozambique Channel Trough [16] equally play vital roles in rainfall extremes in the sub-regions in southern Africa. During austral winter (JJA) when the ITCZ tracks northward, the subtropical semi-permanent high-pressure system migrates northward over the southern African landmasses and the adjacent oceans, resulting in large-scale subsidence. Thus, austral winter is relatively the driest period in large parts of southern Africa.

Studies have examined the relationship between climate drivers, such as the Southern Annular mode (SAM) [17,18], El Niño Southern Oscillation (ENSO) [19–21], and southern African rainfall. Also, the majority of the studies on the relationship between large-scale processes and the seasonal rainfall variability in Zimbabwe are based on teleconnection patterns [22] that rather have a remote influence on the hydroclimate of Zimbabwe. No study has addressed how regional circulation types (modulated by climate drivers such as ENSO and the SAM) in Africa south of the equator, relate to

rainfall patterns over the Zimbabwe landmass. Thus, given the vulnerability of Zimbabwe to flood and drought, which can be exacerbated by global warming, this study will contribute to enhancing the predictability of rainfall in Zimbabwe from the aspect of synoptic climatology.

This study is structured as follows: data and methods are presented in Section 2; the results are presented and discussed in Section 3; conclusions are drawn in Section 4.

2. Materials and methods

Figure A1 shows the spatial map of Zimbabwe, the location in Africa, and the digital elevation model map. The topography consists of a high plateau with mountains in the northeastern regions.

For the classification of circulation patterns in southern Africa and analysis of the associated moisture flux patterns, wind vectors, specific humidity at 850 hPa (i.e., the height above the escarpment in the eastern part of southern Africa), and sea level pressure (SLP) data sets were obtained from ERA5 [23] at a horizontal resolution of 0.25° longitude and latitude. Precipitation data was obtained for Zimbabwe from the Climate Prediction Centre (CPC) [24]. The horizontal resolution of the CPC data is 0.5° longitude and latitude. The temporal resolution at which the data sets were obtained is daily from 1979–2020.

The spatial extent for classifying the circulation types (CTs) in the study region is 0°–50.25° S and 5.75°–55.25° E. It includes the adjacent oceans which act as moisture sources for the landmasses. The classification of the data sets was made using the fuzzy (i.e., a variable can be assigned to more than one class based on some probability of group membership) obliquely rotated principal component analysis (PCA) applied to the T-mode matrix (i.e., variable is time series and observation is grid point) of daily z-score standardized SLP field [25,26]. R studio was used for programming the methods as described in this section. Also the method for classifying the CTs is the same as used by Ref [25], the only difference in this current research is the criterion used in selecting the optimal number of principal components (PCs) to retain, that is, retaining only PCs that resemble the similarity matrix from which they are drawn [26].

Singular value decomposition was used to factorize the correlation matrix relating the daily time series. From the matrix factorization, the eigenvectors, eigenvalues, and PC scores were obtained. The eigenvectors were multiplied by the square root of their corresponding eigenvalues; this makes them longer than a unit length, referred to as PC loadings. The PC loadings are time series and they localize in time the spatial patterns obtained by the PC scores. The number of components to retain was based on matching the rotated PC loadings to the correlation vector that indexes the highest loading magnitude on that particular PC. Only rotated PC loadings that have congruence matches of at least 0.92 with the correlation patterns were retained. As explained by Ref [26], the rotated PC loadings that match well with the correlation structure are designated to be the most physically interpretable PCs that are less contaminated with noise.

The PC loadings were rotated iteratively, keeping 2–20 PCs and the congruence coefficients are calculated at each step to determine the goodness-of-match between the rotated PCs and the correlation patterns. PC rotation can be carried out using Oblique or orthogonal rotation algorithms. Orthogonal rotations (e.g., with Varimax) do not allow correlation between the PC scores while oblique rotations (e.g., with Promax) allows inter-correlation between the PC scores. Since actual atmospheric processes are not orthogonal, inter-correlation between the PC scores is desirable. In this work, a more oblique Promax solution that rotates the loadings to bestfit with the correlations was

reached at a Promax power of 4 (i.e., the power at which the Varimax solution is raised). The rotation maximizes the number of near-zero loadings so that each retained component clusters a unique number of days with a similar spatial pattern. A hyperplane width threshold of ±0.2 was used to separate loadings within the zero interval (i.e., noise) from the signal. Hence for each retained component, loadings greater than or less than ±0.2 [27] form 2 asymmetric classes, and the mean SLP of the days in a given class is the CT. Since atmospheric circulation is fuzzy and continuous, overlapping of the classification is allowed so that a day can be assigned to more than one CT insofar that the day in question has loadings in the signal range (i.e., >0.2) under the corresponding CTs.

Moisture flux, calculated as the product of specific humidity and wind speed at 850 hPa, was used to study moisture advection processes during the active period of the CTs. Hence composites of SLP and moisture flux were used to analyze the advective flow patterns under each CT. The flow patterns were further related to precipitation formation in Zimbabwe.

3. Results and discussion

3.1. Seasonal climatology of rainfall in Zimbabwe

Figure 1 shows the seasonal rainfall totals in Zimbabwe from the CPC data. Austral summer (DJF) is relatively the wettest season and austral winter (JJA) is relatively the driest season. For the transition seasons, the months of March and November are relatively wettest (Figure 2). On the spatial scale, during DJF, the northeastern regions receive higher rainfall amounts compared to the southwestern regions. Throughout the year, the east-central regions tend to be relatively wet. In the calendar month, Figure 2b shows that averaged over Zimbabwe, extreme precipitation relatively prevails during the months of January and February. Also, Figure 2b shows that averaged over Zimbabwe, precipitation is most variable during November to February and least variable, from March to September. In the next section, a further time decomposition of the precipitation data series using CTs will aid in further understanding of the within-season synoptic-scale signals associated with the seasonal spatial rainfall patterns presented in Figure 1.

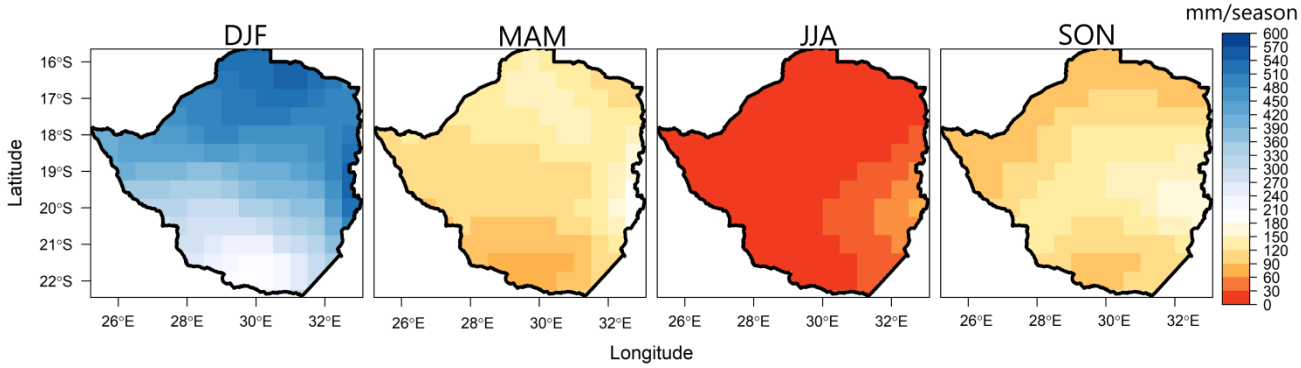

Figure 1. Seasonal precipitation totals over Zimbabwe from the CPC data. The analysis period is 1981 to 2010.

a)

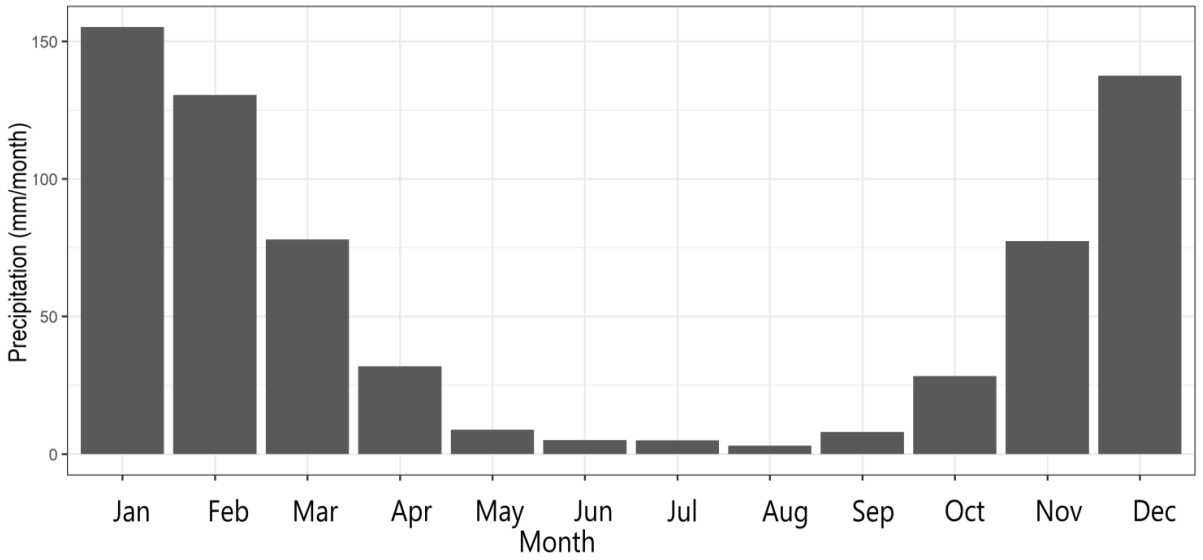

b)

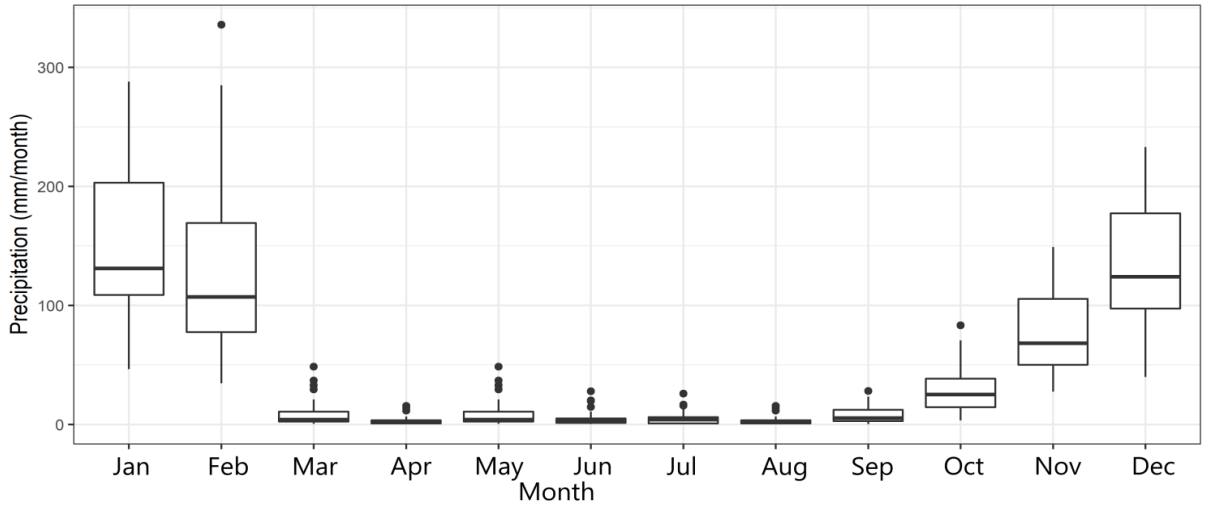

Figure 2. Annual cycle of precipitation averaged over Zimbabwe (a), and the monthly distribution of precipitation averaged over Zimbabwe (b). The analysis period is 1981 to 2010.

3.2. Linkage between moisture circulation and rainfall distribution over Zimbabwe

From the congruence match between the rotated PC loadings and the correlation vectors, the first four PCs match the correlation patterns with a congruence match greater than or equal to 0.92, thus they are retained and analyzed as the leading modes of atmospheric circulation in Africa south of the equator.

Figure 3 shows the SLP and 850 hPa moisture flux composites of the classified CTs. Since four components are retained, eight classes (i.e., CTs) are obtained, which are days with loading magnitudes above and below the ±0.2 threshold under each retained PC. The SLP and 850 hPa moisture flux composite of the days are shown in Figure 3. Furthermore, Figure 4 shows the

resulting patterns of precipitation over Zimbabwe associated with large-scale circulation patterns in Figure 3. Thus, Figure 3 and Figure 4 will be interpreted accordingly in terms of the physical relationship between the mechanism of the CTs and the spatial distribution (and intensity) of precipitation over Zimbabwe. Table 1 also shows the dominant period of the CTs in addition to the spatial average of precipitation over Zimbabwe under each CT.

Based on Figure 4 and Table 1, a further subjective classification of the CTs into relatively wet and relatively dry CTs, over Zimbabwe, will result in CT1−, CT2+, CT3+, and CT4− being grouped as wet CTs. On the other hand, CT1+, CT3− and CT4+ can be grouped as dry CTs. CT2− is more of a transition pattern considered to be in between being wet and dry. CT1− is the wettest CT and CT3− is the driest CT.

Table 1. Spatial average of precipitation in Zimbabwe and dominant periods for each of the classified CTs.

CT	Precipitation average in Zimbabwe (mm/day)	Dominant months
1+	1.56	May to September
1−	2.61	October to April
2+	2.26	February to April
2−	1.74	May to January
3+	2.13	October, November, January to April
3−	1.17	December, May to September
4+	1.27	May to September
4−	2.08	October to April

3.2.1. Circulation patterns linked to wet conditions in Zimbabwe

The wet CTs have relatively higher precipitation amounts at each grid box in Zimbabwe and are generally dominant from middle/late austral spring to early/middle austral autumn (i.e., October to April). SST peaks in the southwest Indian Ocean during austral summer to early/middle austral autumn, given the high heat capacity of the (ocean) water [13]. Thus, the dominant period of the wet CTs (i.e., CT1−, CT2+, CT3+, and CT4−) correlates to when warm SST occurs in the southwest Indian Ocean. Warm SST in the southwest Indian implies that cyclonic activity (i.e., enhanced moist convection) is enhanced over the Oceans, as evident in Figure 4 (i.e., SLP isopleths, considered cyclonic, extend from the tropics towards the Mozambique Channel) for the wet CTs. During late austral spring to early austral autumn, the ITCZ migrates southward, and so does the region of maximum heating. Resultantly, in climatology, the semi-permanent high-pressure systems migrate southward and so the Southern Hemisphere mid-latitude cyclones move poleward. The southward migration of the semi-permanent high-pressure systems limits subsidence over the southern African landmasses and adjacent Oceans [12]; this enables vertical movement favorable for rainfall formation.

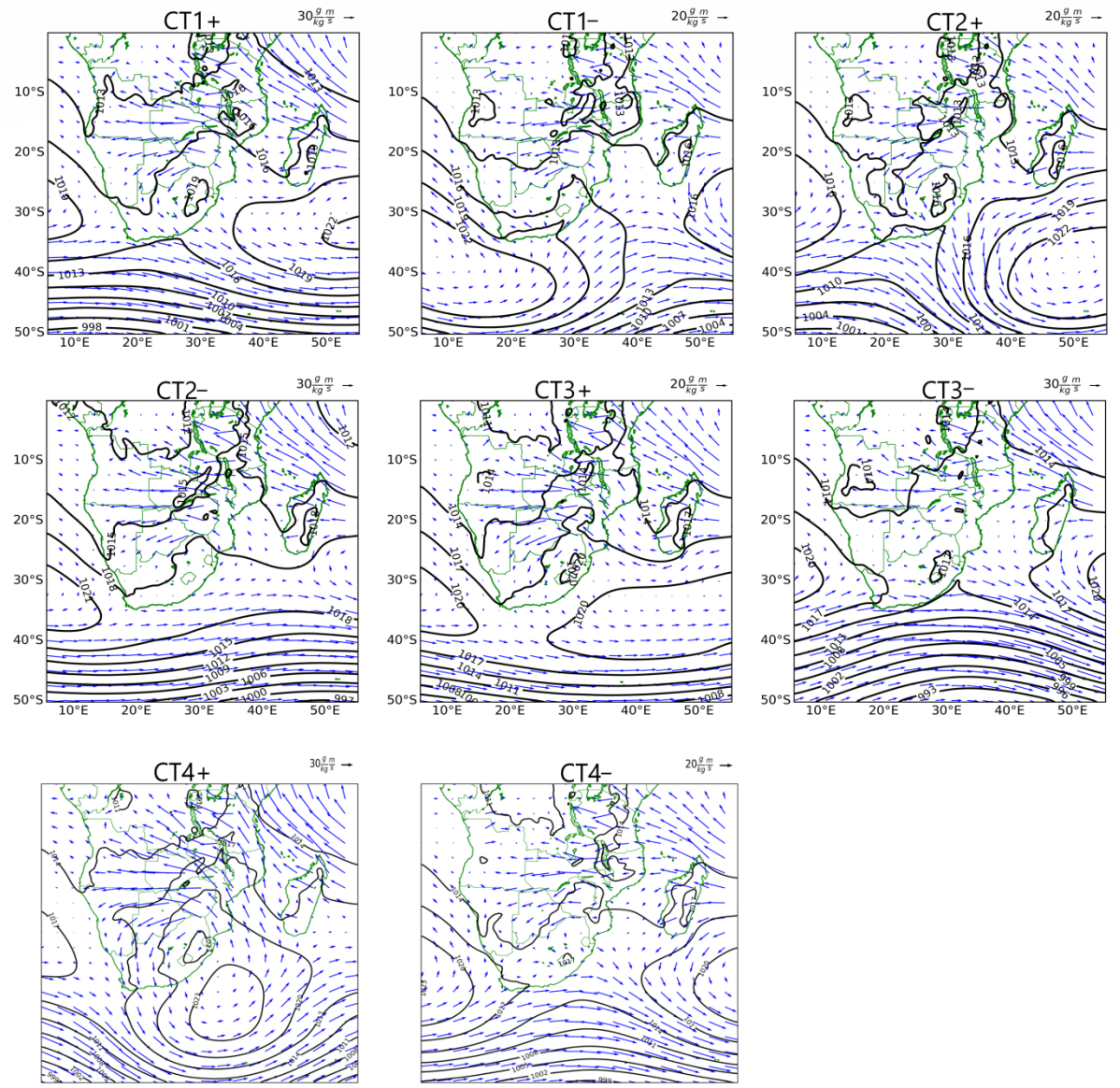

Figure 3. Composites of moisture flux at 850 hPa (blue vectors) and SLP (black contours) for the classified circulation types.

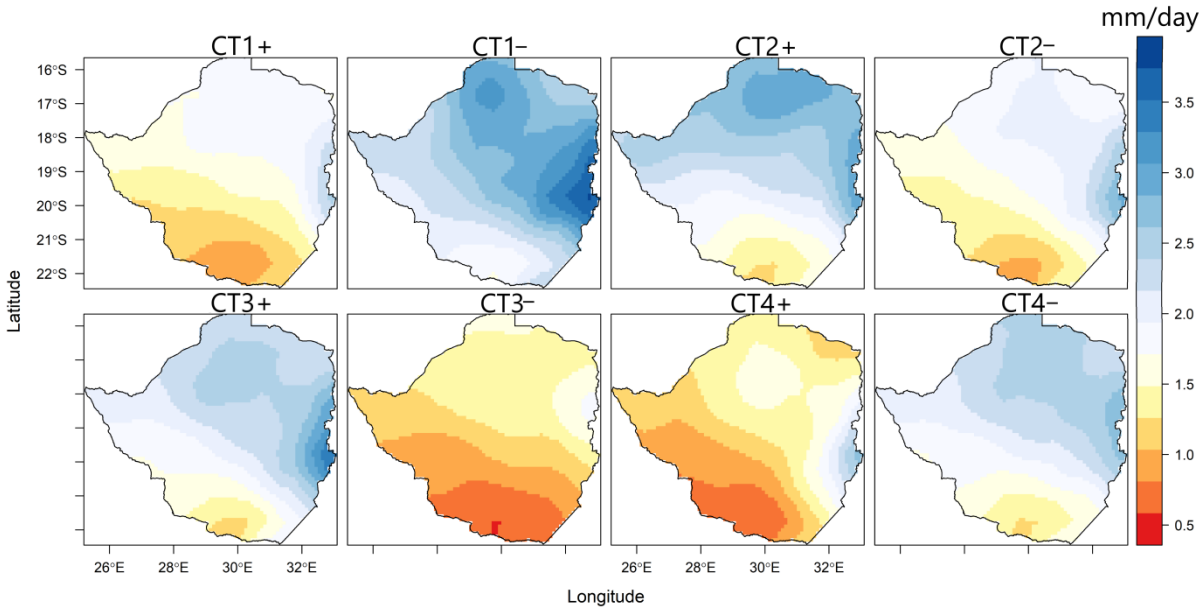

Figure 4. Precipitation composites of the classified circulation types.

From Figure 3, for the wet CTs, CT1− and CT3+ indicates warm-season synoptic states associated with enhanced blocking of the Southern Hemisphere mid-latitude cyclones. A previous study [17] found that CT3+ is related to the Positive SAM phase. During CT1−, the South Atlantic Ocean high-pressure ridges south of South Africa. This triggers a pressure gradient between the ridging high-pressure system and the surface low over the subcontinent. The result is a nearly perpendicular onshore transport of abundance of moisture (from the southwest Indian Ocean) along the eastern coast by southeast winds [27]. Figure 4 shows that this circulation pattern is associated with widespread enhanced rainfall over Zimbabwe.

Under CT3+, the circulation at the western branch of the south Indian Ocean high pressure is enhanced in driving moist southeast winds into southern Africa. However, the high that ridges into the eastern parts of southern Africa, with the inclusion of central to southern Zimbabwe, results in rainfall suppression over southern Zimbabwe due to subsidence (Figure 4). From Figure 4, enhanced rainfall formation under CT3+ is limited to the northeastern regions.

CT2+ and CT4− present synoptic states associated with the northward track Southern Hemisphere mid-latitude cyclones, south of South Africa, during austral warm seasons. The major difference between the two CTs is that the western branch of the South Indian Ocean high pressure is strengthened (weakened) under CT2+ (CT4−). With the northward track of the Southern Hemisphere mid-latitude cyclones, in addition to weakening of the western branch of the South Indian Ocean high pressure, under CT4−, westerlies rather prevail south of South Africa and over parts of the southwest Indian Ocean. Also, since the South Indian Ocean high pressure is more eastward, the resulting southeast winds are obstructed by the Madagascar topography. Thus, under CT4−, low-level advective flow into Zimbabwe, from the southwest Indian Ocean is low. However, from Figure 3, the extent of cyclonic/convective activity in the southwest Indian Ocean, or specifically the Mozambique Channel, is highest under CT4− (i.e., the extent to which the SLP isopleths from the tropics extends to the Mozambique Channel). CT4− reveals that during austral warm seasons, even

when southeast advective flow into Zimbabwe is weakened, enhanced convective activity (implying enhanced moisture availability) in the southwest Indian Ocean can still result in rainfall formation over (northern) parts of Zimbabwe (Figure 4).

CT2+ indicates that when the anticyclonic circulation at the western branch of the South Indian Ocean high-pressure is strong and not ridging into the eastern parts of southern Africa (like in CT3+), the enhanced southeasterly fluxes can be partly constrained by the westerly fluxes associated with an enhanced state of the mid-latitude cyclones. Thus, moisture penetration into Zimbabwe, from the southwest Indian Ocean, is limited compared to CT1−.

3.2.2. Circulation patterns linked to dry conditions over Zimbabwe

For the dry CTs (i.e., CT1+, CT3− and CT4+) the dominant periods are generally from late austral autumn to early austral spring (i.e., May to September). These periods are characterized by the northward migration of the ITCZ and the semi-permanent high-pressure systems, resulting in subsidence over southern Africa and the adjacent Oceans. Hence, SST is expected to be cooler (compared to the summer months) during late austral autumn to early austral spring. From Figure 3, it is evident that for the dry CTs, anticyclonic activity dominates over southern Africa (i.e., the SLP isopleths from the semi-permanent high-pressure systems, considered to be anti-cyclonic, extend over the southern landmasses and adjacent oceans). The implications are subsidence over the southern parts of Zimbabwe, resulting in why in Figure 4, the southern parts are relatively drier in all the (dry) CTs; and strong winds—that are relatively drier compared to warmer seasons. However, given the high specific heat capacity of ocean water, the southwest Indian Ocean is expected to retain some moisture relative to the South Atlantic Ocean (i.e., around the cold Benguela current). This is because the southwest Indian Ocean is geographically characterized by the warm Mozambique current and Agulhas current, and the typical presence of the ITCZ during the warmer season. Under CT4+ large parts of southern Africa and the greater Agulhas region are dominated by an anticyclone (Figure 3). Nonetheless, the associated enhanced southeast winds lead to wetter conditions on the east coast of Zimbabwe (Figure 4).

CT1+ and CT3− are similar synoptic conditions associated with the northward track of the Southern Hemisphere mid-latitude cyclone. CT3− is related to the negative phase of the SAM [17]. However, the strength, horizontal and vertical extent (i.e., towards the equator) of the Southern Hemisphere mid-latitude cyclones is highest under CT3−. With the inclusion of the impact of the Madagascar topography in blocking southeast moisture fluxes towards southern Africa, advective flow from the southwest Indian Ocean into Zimbabwe is lowest under CT3−, resulting in why it is the driest CT. Thus, the negative SAM can contribute to dry conditions in Zimbabwe through its control of CT3−. Moreover, the wet and dry CTs also influence pollutant concentrations in Zimbabwe. For example, during the winter season, Figure A2 shows that the asymmetries of CT3+/CT3− and CT4+/CT4− (Figure 3) implies that enhanced easterly/westerly winds over the southwest Indian Ocean can contribute to lower/higher concentrations of Particulate matter with diameter less than 2.5 (PM2.5) at preferred regions, over Zimbabwe. Higher concentrations of PM2.5 can results to respiratory and cardiovascular diseases [28]; Figure A2 and Figure 3 indicate that at the synoptic scale, strong and moist easterly winds are necessary in reducing PM2.5 concentrations at preferred regions in Zimbabwe.

3.2.3. Synoptic pattern during the 22 February flood episode in Zimbabwe

Rainfall variability at the eastern coastal landmass of southern Africa is influenced by tropical cyclones in the Mozambique Channel [29]. During tropical cyclone events in the Mozambique Channel, weakening of atmospheric blocking by the western branch of the south Indian Ocean high-pressure, coupled with enhanced cyclonic activity in the southwest Indian Ocean implies that the tropical cyclone will tend to progress further south and can be steered into the coastal landmasses by northeast winds [30–32]. On 22 February 2000, Zimbabwe was hit by tropical cyclone Eline, causing devastating conditions, especially in the eastern and southern parts of the country [33]. Figure 5 shows the SLP and 850 hPa moisture composite from 21 to 23 February 2000. The synoptic features involve (i) a ridging South Atlantic Ocean anticyclone south of South Africa, (ii) a weaker and more eastward state of the South Indian Ocean high-pressure, and (iii) enhanced cyclonic activity in the southwest Indian Ocean. Since tropical cyclones tends to move towards the regions with low pressure, coupled with the northeast winds, these synoptic conditions are favorable for the cyclone to steer southwest into the eastern coastal landmasses. Ref [34] reported that the co-occurrence of a tropical low coupled with a ridging anticyclone can be responsible for heavy rainfall over the eastern coastal regions of southern Africa. Several other studies have equally noted that the eastward extension of a closed South Atlantic Ocean high-pressure system is important to the synoptic climatology of South Africa and other countries on the east coast of southern Africa [35–37]. As shown under CT1− in Figure 3 and Figure 5 during tropical cyclone Eline, the eastward extension of a closed South Atlantic Ocean high-pressure system, normally co-occurs with a more eastward positioning of the Mascarene high. Resultantly, atmospheric blocking of tropical cyclones that form around the Mozambique Channel is weakened, and this creates a favorable atmospheric condition that allows the tropical cyclonic system to penetrate Zimbabwe.

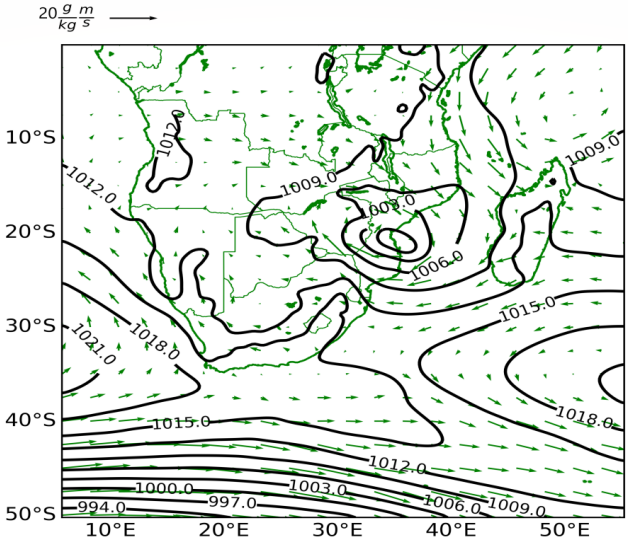

Figure 5. Composites of moisture flux at 850 hPa (green vectors) and SLP (black contours) for 21 to 23 February 2000 when CT4− and CT1− occurred according to the classification scheme. The Contour interval is 3 hPa.

4. Conclusions

The relationship between the patterns of atmospheric circulation in Africa south of the equator and the spatial distribution of rainfall in Zimbabwe is examined in this study. It was found that during the austral summer season, widespread wet conditions over Zimbabwe can be linked to the ridging of the South Atlantic Ocean high-pressure south of South Africa. This implies both the further poleward displacement of the Southern Hemisphere mid-latitude cyclones, a more eastward positioning of the Western branch of the Mascarene high and enhanced onshore southeast moisture fluxes, from the southwest Indian Ocean to the east coast of southern Africa. Conversely, a widespread dry condition in Zimbabwe was found to be linked to the northward track of the Southern Hemisphere mid-latitude cyclones. This leads to both enhanced subsidence over (southern) Zimbabwe and enhanced westerly moisture fluxes (that limit southeast advective flow) from the southwest Indian Ocean.

Finally, the relationship between synoptic circulations and regional rainfall can be subjected to changes in the climate system as a result of natural climate variability (e.g., [38,39]) and anthropogenic induced climate change [40]. Therefore, it is necessary to investigate how atmospheric forcing due to anomalies in climate drivers and anthropogenic climate change impact the mechanisms of the CTs in this work, and the resulting influence on the intensity and spatial distribution of rainfall in Zimbabwe.

Data availability

ERA5 datasets are available at https://climate.copernicus.eu/climate-reanalysis. The CPC data is available at https://psl.noaa.gov/data/gridded/data.ncep.reanalysis.html (accessed on 5 October 2021).

Conflict of interest

The authors declare no conflict of interest.

References

1. AfDB (2011) Infrastructure and growth in Zimbabwe: an action plan for sustained strong economic growth. Summary Report. Available from: https://www.afdb.org/fileadmin/uploads/afdb/Documents/Generic-Documents/1.%20Standalone%20Summary%20Report.pdf
2. Unganai L (2009) Adaptation to climate change among agropastoral systems: case for Zimbabwe. *IOP Conf Ser Earth Environ Sci* 6: 412045. https://doi.org/10.1088/1755-1307/6/41/412045
3. Mutasa C (2008) Evidence of climate change in Zimbabwe: paper presented at the climate change awareness and dialogue. Workshop for Mashonaland Central and Mashonaland West Provinces held at Caribbea Bay Hotel, Kariba, Zimbabwe. 29–30 September.
4. GoZ (2010) Medium term plan, January 2010–December 2015. Government of Zimbabwe, Ministry of Economic Planning and Investment Promotion, Harare.

5. Chagutah T (2010) Climate change vulnerability and preparedness in Southern Africa: Zimbabwe Country Report. Heinrich Boell Stiftung, Cape Town.
6. IPCC (2007) *Climate Change 2007—Impacts, Adaptation and Vulnerability: Working Group II Contribution to the Fourth Assessment Report of the Intergovernmental Panel on Climate Change*, Cambridge, UK: Cambridge University Press, 469–506. Available from: https://www.ipcc.ch/site/assets/uploads/2018/03/ar4_wg2_full_report.pdf.
7. WFP (2019) How drought is killing Zimbabwe. Available from: https://www.wfp.org/stories/how-drought-killing-zimbabwe.
8. Nyahunda L, Tirivangasi HM (2021) Barriers to Effective Climate Change Management in Zimbabwe's Rural Communities. *African Handbook of Climate Change Adaptation*. Springer, Cham. https://doi.org/10.1007/978-3-030-45106-6_251
9. Cook KH (2000) The South Indian convergence zone and interannual rainfall variability over Southern Africa. *J Climate* 13: 3789–3804. https://doi.org/10.1175/1520-0442(2000)013<3789:TSICZA>2.0.CO;2
10. Macron C, Pohl B, Richard Y, et al. (2014) How do tropical-temperate troughs form and develop over southern Africa? *J Climate* 27: 1633–1647. https://doi.org/10.1175/JCLI-D-13-00175.1
11. Hart NC, Reason CJC, Fauchereau N (2012) Cloud bands over southern Africa: seasonality, contribution to rainfall variability and modulation by the MJO. *Clim Dynam* 41: 1199–1212. https://doi.org/10.1007/s00382-012-1589-4
12. Vigaud N, Richard Y, Rouault M, et al. (2009) Moisture transport between the South Atlantic Ocean and Southern Africa: relationships with summer rainfall and associated dynamics. *Clim Dynam* 32: 113–123. https://doi.org/10.1007/s00382-008-0377-7
13. Reason CJC, Mulenga H (1999) Relationships between South African rainfall and SST anomalies in the southwest Indian Ocean. *Int J Climatol* 19: 1651–1673. https://doi.org/10.1002/(SICI)1097-0088(199912)19:15<1651::AID-JOC439>3.0.CO;2-U
14. Munday C, Washington R, Hart N (2020) African low-level jets and their importance for water vapor transport and rainfall. *Geophys Res Lett* 48: e2020GL090999. https://doi.org/10.1029/2020GL090999
15. Ibebuchi CC (2022) Circulation patterns linked to the positive sub-tropical Indian Ocean dipole. *Adv Atmos Sci*. https://doi.org/10.1007/s00376-022-2017-2
16. Barimalala R, Blamex RC, Desbiolles F, et al. (2020) Variability in the Mozambique Channel Trough and impacts on Southeast African rainfall. *J Climate* 33: 749–765. https://doi.org/10.1175/JCLI-D-19-0267.1
17. Ibebuchi CC (2021) On the relationship between circulation patterns, the southern annular Mode, and rainfall variability in Western Cape. *Atmosphere* 12: 753. https://doi.org/10.3390/atmos12060753
18. Reason CJC, Rouault M (2005) Links between the Antarctic Oscillation and winter rainfall over western South Africa. *Geophys Res Lett* 32. https://doi.org/10.1029/2005GL022419
19. Richard Y, Trzaska S, Roucou P, et al. (2000) Modification of the southern African rainfall variability/ENSO relationship since the late 1960s. *Clim Dynam* 16: 883–895. https://doi.org/10.1007/s003820000086
20. Dieppois B, Rouault M, New M (2015) The impact of ENSO on southern African rainfall in CMIP5 ocean atmosphere coupled climate models. *Clim Dynam* 45: 2425–2442. https://doi.org/10.1007/s00382-015-2480-x

21. Ibebuchi CC (2021) Revisiting the 1992 severe drought episode in South Africa: the role of El Niño in the anomalies of atmospheric circulation types in Africa south of the equator. *Thero Appl Climatol* 146: 723–740. https://doi.org/10.1007/s00704-021-03741-7
22. Mamombe V, Kim WM, Choi YS (2017) Rainfall variability over Zimbabwe and its relation to large-scale atmosphere-ocean processes. *Int J Climatol* 37: 963–971. https://doi.org/10.1002/joc.4752
23. Hersbach H, Bell B, Berrisford P, et al. (2020) The ERA5 global reanalysis. *Q J R Meteor Soc* 146: 1999–2049. https://doi.org/10.1002/qj.3803
24. Xie P, Chen M, Yang S, et al. (2007) A gauge-based analysis of daily precipitation over East Asia. *J Hydrometeorol* 8: 607–626. https://doi.org/10.1175/JHM583.1
25. Ibebuchi CC (2021) Circulation pattern controls of wet days and dry days in Free State, South Africa. *Meteorol Atmos Phys* 133: 1469–1480. https://doi.org/10.1007/s00703-021-00822-0
26. Richman MB (1981) Obliquely rotated principal components: an improved meteorological map typing technique? *J Appl Meteorol Clim* 20: 1145–1159. https://doi.org/10.1175/1520-0450(1981)020<1145:ORPCAI>2.0.CO;2
27. Gong X, Richman MB (1995) On the application of cluster analysis to growing season precipitation data in North America east of the rockies. *J Climate* 8: 897–931. https://doi.org/10.1175/1520-0442(1995)008<0897:OTAOCA>2.0.CO;2
28. Xing YF, Xu YH, Shi MH, et al. (2016) The impact of PM2.5 on the human respiratory system. *J Thorac Dis* 8: E69–E74. https://doi.org/10.3978/j.issn.2072-1439.2016.01.19
29. Uele DL, Lyra GB, De Oliveira Júnior JF (2017) Spatial and intrannual variability of rainfall in south region of the Mozambique, Southern Africa. *Rev Bras Meteorol* 32: 473–484. https://doi.org/10.1590/0102-77863230013
30. Ndarana T, Bopape MJ, Waugh D, et al. (2018) The influence of lower stratosphere on ridging Atlantic Ocean Anticyclone over South Africa. *J Climate* 31: 6175–6187. https://doi.org/10.1175/JCLI-D-17-0832.1
31. Reason CJC (2007) Tropical cyclone Dera, the unusual 2000/01 tropical cyclone season in the South West Indian Ocean and associated rainfall anomalies over Southern Africa. *Meteorol Atmos Phys* 97: 181–188. https://doi.org/10.1007/s00703-006-0251-2
32. Ibebuchi CC (2022) Can synoptic patterns influence the track and formation of tropical cyclones in the Mozambique Channel? *AIMS Geosci* 8: 33–51. https://doi.org/10.3934/geosci.2022003
33. UNCT Zimbabwe (2020) Floods disaster in Zimbabwe. Available from: https://reliefweb.int/report/zimbabwe/floods-disaster-zimbabwe.
34. Crimp SJ, Mason SJ (1999) The extreme precipitation event of 11 to 16 February 1996 over South Africa. *Meteorol Atmos Phys* 70: 29–42. https://doi.org/10.1007/s007030050023
35. Jury MR (2015) Passive suppression of South African rainfall by Agulhas current. *Earth Interact* 19: 1–14. https://doi.org/10.1175/EI-D-15-0017.1
36. Engelbrecht CJ, Landman WA, Engelbrecht FA, et al. (2015) A synoptic decomposition of rainfall over the Cape south coast of South Africa. *Clim Dynam* 44: 2589–2607. https://doi.org/10.1007/s00382-014-2230-5
37. Stander JH, Dyson L, Engelbrecht CJ (2016) A snow forecasting decision tree for significant snowfall over the interior of South Africa. *S Afr J Sci* 112: 1–10. https://doi.org/10.17159/sajs.2016/20150221
38. De Oliveira-Júnior JF, Shah M, Abbas A, et al. (2022) Spatiotemporal analysis of drought and

rainfall in Pakistan via Standardized Precipitation Index: homogeneous regions, trend, wavelet, and influence of El Niño-southern oscillation. *Theor Appl Climatol* 149: 843–862. https://doi.org/10.1007/s00704-022-04082-9

39. Zeri M, Cunha-Zeri G, Gois G, et al. (2019) Exposure assessment of rainfall to interannual variability using the wavelet transform. *Int J Climatol* 39: 568–578. https://doi.org/10.1002/joc.5812
40. Correia Filho WLF, De Oliveira-Júnior JF, De Barros Santiago D, et al. (2019) Rainfall variability in the Brazilian northeast biomes and their interactions with meteorological systems and ENSO via CHELSA product. *Big Earth Data* 3: 315–337. https://doi.org/10.1080/20964471.2019.1692298

Appendix

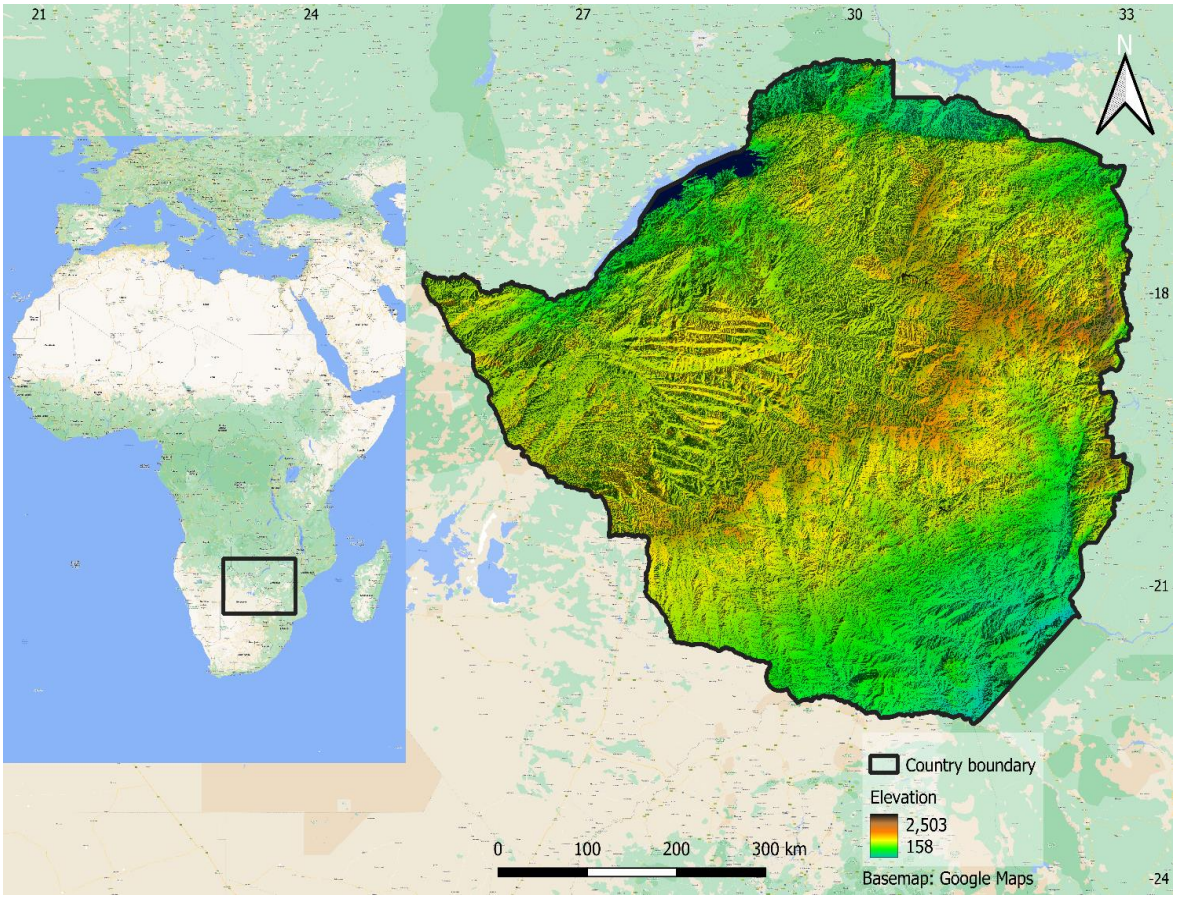

Figure A1. Location of Zimbabwe in Africa (black frame) and the digital elevation model map of Zimbabwe.

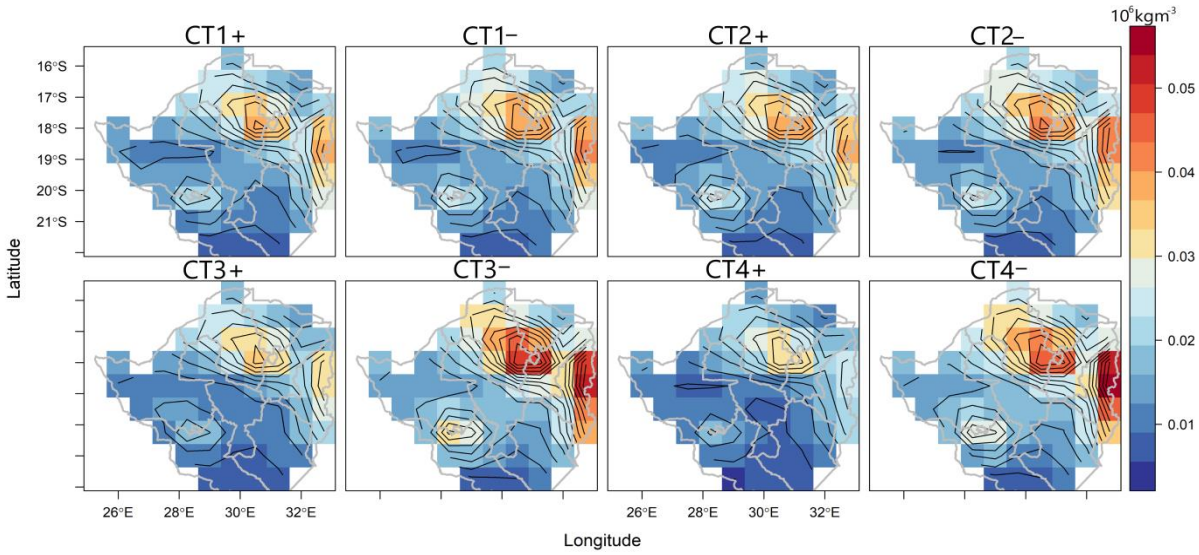

Figure A2. PM 2.5 composites during the classified circulation types in Figure 3, for the winter season.